Since January 2020 Elsevier has created a COVID-19 resource centre with free information in English and Mandarin on the novel coronavirus COVID-19. The COVID-19 resource centre is hosted on Elsevier Connect, the company's public news and information website.

Elsevier hereby grants permission to make all its COVID-19-related research that is available on the COVID-19 resource centre - including this research content - immediately available in PubMed Central and other publicly funded repositories, such as the WHO COVID database with rights for unrestricted research re-use and analyses in any form or by any means with acknowledgement of the original source. These permissions are granted for free by Elsevier for as long as the COVID-19 resource centre remains active.

Informatics in Medicine Unlocked 23 (2021) 100541

Contents lists available at ScienceDirect

Informatics in Medicine Unlocked

journal homepage: http://www.elsevier.com/locate/imu

Repurposing FDA-approved drugs to fight COVID-19 using *in silico* methods: Targeting SARS-CoV-2 RdRp enzyme and host cell receptors (ACE2, CD147) through virtual screening and molecular dynamic simulations

Soodeh Mahdian [a], Mahboobeh Zarrabi [b,*], Yunes Panahi [c], Somayyeh Dabbagh [b]

[a] Department of Cellular and Molecular Biology, Faculty of Biological Sciences, North Tehran Branch, Islamic Azad University, Tehran, Iran
[b] Department of Biotechnology, Biological Faculty, Alzahra University, Tehran, Iran
[c] Pharmacotherapy Department, Faculty of Pharmacy, Baqiyatallah University of Medical Sciences, Tehran, Iran

ARTICLE INFO

Keywords:
COVID-19
CD147
ACE2
RdRp
Drug repurposing

ABSTRACT

Background: Different approaches have been proved effective for combating the COVID-19 pandemic. Accordingly, *in silico* drug repurposing strategy, has been highly regarded as an accurate computational tool to achieve fast and reliable results. Considering SARS-CoV-2's structural proteins and their interaction the host's cell-specific receptors, this study investigated a drug repurposing strategy aiming to screen compatible inhibitors of FDA-approved drugs against viral entry receptors (ACE2 and CD147) and integral enzyme of the viral polymerase (RdRp).

Methods: The study screened the FDA-approved drugs against ACE2, CD147, and RDRP by virtual screening and molecular dynamics (MD) simulation.

Results: The results of this study indicated that five drugs with ACE2, four drugs with RDRP, and seven drugs with CD147 achieved the most favorable free binding energy ($\Delta G < -10$). This study selected these drugs for MD simulation investigation whose results demonstrated that ledipasvir with ACE2, estradiol benzoate with CD147, and vancomycin with RDRP represented the most favorable ΔG. Also, paritaprevir and vancomycin have good binding energy with both targets (ACE2 and RdRp).

Conclusions: Ledipasvir, estradiol benzoate, and vancomycin and paritaprevir are potentially suitable candidates for further investigation as possible treatments of COVID-19 and novel drug development.

1. Introduction

Since the outbreak of the COVID-19 pandemic in late 2019, many have attempted to find a reliable treatment. Based on the reports of WHO, more than 17 million global cases have been confirmed thus far [1]. Given the data on structural properties of SARS-CoV-2, the causative agent of the COVID-19, and its homology to beta-coronaviruses of familiar viruses, such as SARS and MERS, similar therapeutic strategies have thus far been applied [2]. However, no effective drug has yet been introduced to treat and combat specific structures of viral components, despite the prescription of various medications, including hydroxychloroquine [3], azithromycin [4], remdesivir [5], idasanutlin [6], and favipiravir [7]. Therefore, pharmacological studies concerning COVID-19 treatment are still in progress. Many research studies have addressed the COVID-19 treatment, focusing on the drug repurposing technique for implementing which recognizing pathogenic targets is essential. In this case, biological insights toward genomic and structural properties of SARS-CoV-2 have identified many features of viral pathogenic targets [8]. RNA-dependent RNA polymerase (RdRp) is integral for preserving viral life, and several reports indicate that positive-sense viruses have conserved RdRp enzymes [9]. In line with these findings, X-ray crystallography and structural properties of SARS-CoV-2 RdRp were conducted to introduce novel antiviral drug designs and drug repurposing approaches [10]. Spike glycoprotein, as a structural protein of SARS-CoV-2, plays a critical role in the initial steps of pathogenesis. Structural studies and biochemical experiments have confirmed the binding of SARS-CoV2 spike to human angiotensin-converting enzyme (ACE2) receptors [11]. According to these studies, receptor-binding

* Corresponding author.
E-mail address: mzarrabi@alzahra.ac.ir (M. Zarrabi).

https://doi.org/10.1016/j.imu.2021.100541
Received 17 December 2020; Received in revised form 19 February 2021; Accepted 20 February 2021
Available online 25 February 2021
2352-9148/© 2021 The Author(s). Published by Elsevier Ltd. This is an open access article under the CC BY license (http://creativecommons.org/licenses/by/4.0/).

domains (RBD) of the spike undergo transient movements that trigger further up and down conformations for receptor attachment [12]. Based on surface Plasmon resonance studies, ACE2 binds to the RBD of SARS-CoV-2 spike with nearly ten to twenty-fold higher affinity than SARS-CoV spike ectodomain [13]. ACE2 is expressed in the lower respiratory tract, skin keratinocytes, small intestine cells, and oral epithelial cells [14]. Furthermore, the expression of ACE2 and the infection severity were correlated *in vitro* [15]. It has been shown that ACE2 expression patterns increase during tumor propagation [16], and factors such as age, diabetes, and cardiovascular diseases also impact expression patterns [17]. Recent studies have revealed functional patterns of CD147 receptor involvement in infection dissemination [18]. CD147 participates in inflammation, nutrient, and drug transporter activity, as well as microbial pathology, and developmental processes. Also, it has efficacy in certain infectious diseases, such as malaria, neisseria meningitides, and HIV-1 [19]. It has been reported that COVID-19 creates a novel route for CD147-spike protein (SP) through which it invades host cells [20]. It is known as Basigin or extracellular matrix metalloproteinase inducer and also a cell receptor in erythrocytes for the parasite *Plasmodium falciparum* [21]. The expression levels of CD147 receptors increase in patients with asthma, making them a susceptible group to SARS-CoV-2 infection [22]. Considering all the above aspects, this study selected RdRp, ACE2, and CD147 and screened them against 2471 FDA-approved libraries by *in silico* methods. The result showed significant binding of many approved small molecules to the chosen targets. Then, the complexes with the top-docked results were simulated for 100 ns to analyze the stability. In such a case, it is possible to repurpose several predicted drugs to prevent and treat SARS-CoV-2.

2. Methods

2.1. System input setup and initial structures

Proteins: It was the ACE2-SARS-CoV-2 RBD complex, as the crystal structure of ACE2 (PDB id: 6M0J), that justified its use in this study [23]. The crystal structure of CD147 (PDB id: 3B5H) at the 2.8 Å resolution provides a suitable structural explanation by homo/hetero-oligomerizations and represents a general structure of other CD147 family members [24]. The predicted structure of RdRp coordinate files was also obtained from the I-TASSER server. The structural PDB files were investigated to detect various problems, such as undesirable HETATOMs, attached ligands, missing atoms, and possible chain breaks. Then, all crystallographic waters were removed from the structures, and molecular hydrogens were added to optimize hydrogen bonds and minimized using the GROMACS 5.1.7 package before docking [25].

Small molecules: The study used the section of small-molecules in the DrugBank database (https://www.drugbank.ca/about) to obtain all FDA-approved drugs [26]. Non-unique structures removed during the process included compounds containing rare atoms and organometallic compounds. Eventually, 2471 compounds were selected.

2.2. Virtual screening

The study used the Pyrx tool for virtual screening [27,28]. The unit-docking cell was defined with Pockdrug server [29] and Uniprot databases. Input pdbqt files for Autodock Vina and minimization steps were generated by the Pyrx tool. Finally, to screen libraries of compounds against targets, the study implemented AutoDock Vina for drug discovery. Docking was done using a 92 Å × 84 Å × 98 Å binding site grid box for ACE2, a 120 Å × 110 Å × 117 Å binding site grid box for CD147 and a 140 Å × 122 Å × 111 Å binding site grid box for RdRp. A total of the top eight poses were retained from the docking run. The interaction established in two dimensions was illustrated in Biovia Discovery Studio, and for 3D visualization of drug/target complexes, Molegro Virtual Docker was used [30].

2.3. Molecular dynamics simulation

The results of virtual screening indicated that five drugs with ACE2, four drugs with RdRp, and seven drugs with CD147 achieved the most favorable free binding energy ($\Delta G < -10$ kcal/mol). For further evaluations, these drugs were chosen for MD simulation to calculate the number of H-bonds and free energy of interaction. MD simulations were directed using the GROMACS 5.1.4 package [31]. The GROMOS 54a7 force field was utilized for the complexes [32]. The study used the ATB server for the preparation of the coordinates and topology of ligands. The study applied appropriate amounts of chloride ions and sodium to all simulation boxes to neutralize the system. Periodic Boundary Condition (PBC) was applied along every simulation box axis, and the SP3 water model was also utilized for system solvation [33] in each simulation system. The LINCS algorithms constrained all covalent bonds. MD simulations were done through a short-range electrostatic interaction as well as a 1.2 nm distance cutoff for the van der Waals interaction. The Particle Mesh Ewald (PME) algorithm calculated the long-range electrostatic interaction. The steepest descent algorithm fulfilled the energy minimization of all systems, and then the NVT ensemble for 500 ps equilibrated all the systems. Then, the NPT ensemble progressively directed the equilibration of each system and the Nose-Hoover algorithm temperature [34,35] was preserved at a temperature of 310 K. During the NPT equilibration, the Parrinello-Rahman barostat [36] maintained the pressures at 1 bar. The MD simulation was completed for the complexes in 100 ns.

2.4. Analyses

The nonpolar and polar interactions between CD147, ACE2, and RdRp with drugs are explainable by binding free-energy calculation. By exercising the MM-PBSA method, the binding free-energy was calculated using the g_mmpbsa tool [37]. The total amount of binding free-energy (ΔG) is realized by adding up the nonpolar interaction free-energy ($\Delta G_{nonpolar}$) and the polar interaction free-energy (ΔG_{polar}) that can be explained as follows:

$$\Delta G_{total} = \Delta G_{nonpolar\ (\Delta G_{nps}+\Delta G_{vdW})} + \Delta G_{polar\ (\Delta G_{ps}+\Delta G_{elec})}$$

Where ΔG_{elec}, ΔG_{ps}, ΔG_{vdW}, ΔG_{nps} are respectively the electrostatic energy, polar solvation energy, van der Waals energy, nonpolar solvation energy.

3. Results

This study applied virtual screening FDA-approved drugs against RdRp, ACE2, and CD147.

3.1. Virtual screening

According to the results, five drugs with ACE2, four drugs with RdRp, and seven drugs with CD147 achieved the most favorable free binding energy (Docking score < -10 kcal/mol) (Table 1). The hydrogen bonding of docked molecules was calculated using Molegro Virtual Docker and Biovia Discovery Studio v.4.5. 2D (Supplementary data).

3.2. Molecular dynamics simulation

MD simulation for all complexes of the ACE2, RDRP, and CD147 with the top-selected drugs is performed for 100 ns. RMSD of alpha carbon atoms, RMSF of all amino acid residues, the number of hydrogen bonds, and free energy of interaction for the drug/protein complexes are investigated.

3.2.1. RMSD and RMSF

Figs. 1A, 2A and 3A depict the RMSD of ACE2, CD147, and RdRp

Table 1
Docking results of FDA-approved drugs and ACE2, CD147 and RdRp with the best binding free energy (Docking score < -10) and the number of hydrogen bonds at 0, 20, 40, 60, 80 and 100 ns. The length of the Hydrogen bond ranges from 2.6 to 3.1 Å.

Complexes	Binding energy (kcal/mol)	H-bond Donor/ acceptor (0, 20, 40, 60, 80 and 100 ns)		H-bond Interactions (Interacting residues) (0, 20, 40, 60, 80 and 100 ns)
ACE2_Paritaprevir	−11.2	0 ns	4	Asn 394, Asp 206, Lys 562, Gln 102
		20 ns	2	Lys 562, Asp 206
		40 ns	3	Lys 562, Asp 206, Gly 104
		60 ns	4	Lys 562, Asp 206, Gly 104, Asn 103
		80 ns	3	Lys 562, Asp 206, Asn 103
		100 ns	4	Lys 562, Asp 206, Gly 104, Asn 103
ACE2_Ledipasvir	−11	0 ns	3	Lys 441, His 378, Glu 402
		20 ns	1	Lys 441
		40 ns	2	Lys 441, Ile 291
		60 ns	2	Lys 441, Arg 273
		80 ns	2	Lys 441, Arg 273
		100 ns	4	Lys 441, Arg 273, His 345, His 505
ACE2_Vancomycin	−10.8	0 ns	4	Asn 117, Asn 103, Tyr 202, Asn 394
		20 ns	5	His 401, His 378, Arg 514, Lys 562, Asn 117
		40 ns	6	Asn 394, Leu 392, Arg 514, Glu 402, Ser 105, Ser 113
		60 ns	9	Lys 562, Glu 398, Asp 206, Gln 102, Lys 187, Ser 105, Ser 70, Tyr 102, Tyr 202
		80 ns	7	Lys 187, Gln 102, Tyr 199, Asp 117, Gly 205,Asn 394, Lys 562
		100 ns	10	Lys 187, Gln 102, Tyr 199, Phe 390, Arg 393, Gln 98, Tyr 196, Asp 509, Asn 117, Tyr 196
ACE2_Sirolimus	−10.7	0 ns	3	Asn 210, Gln 98, Lys 562
		20 ns	2	Lys 94, Asn 210
		40 ns	2	Lys 94, Asn 210
		60 ns	2	Lys 94, Asn 210
		80 ns	2	Lys 94, Asn 210
		100 ns	2	Lys 94, Asn 210
ACE2_Nilotinib	−10.5	0 ns	2	Gln 102, Lys 562
		20 ns	3	Arg 219, Gln 102, Asn 103
		40 ns	1	Gln 102
		60 ns	2	Gln 98, Tyr 196
		80 ns	2	Arg 219, Glu 208
		100 ns	2	Arg 219,Gln 102
CD147-Irinotecan	−11.6	0 ns	2	Glu 64, Glu 73
		20 ns	2	Glu 64, Glu 73
		40 ns	2	Glu 64, Lys 75
		60 ns	2	Glu 64, Lys 36
		80 ns	3	Glu 64, Lys 36, His 53
		100 ns	4	Glu 64, Lys 36, Glu 73, Gln 70
CD147_Abemaciclib	−11.1	0 ns	1	Glu 73
		20 ns	1	Lys 36
		40 ns	0	–
		60 ns	0	–
		80 ns	0	–
		100 ns	1	Glu 64
CD147_Estradiol benzoate	−10.7	0 ns	1	Lys 75
		20 ns	2	Lys 75, Tyr 85
		40 ns	2	Lys 75, Lys 57
		60 ns	3	Lys 75, Lys 57, Glu 73
		80 ns	3	Lys 75, Glu 73, Tyr 85
		100 ns	3	Lys 75, Lys 57, Glu 73
CD147_Capmatinib	−10.7	0 ns		–
		20 ns	3	Lys 36, Lys 57, Asp 80
		40 ns	3	Lys 36, Lys 57, Asp 80
		60 ns	4	Lys 36, Lys 57, Lys 75, Asp 80
		80 ns	4	Lys 36, Lys 57, Asp 80, Tyr 85
		100 ns	3	Lys 36, Lys 57, Asp 80
CD147_Olaparib	−10.6	0 ns	1	Lys 75
		20 ns	1	Lys 57
		40 ns	2	Lys 57, Glu 64
		60 ns	4	Lys 75, Lys 57, Glu 64, Tyr 85
		80 ns	4	Lys 57, Glu 73, Lys 36, Asp 77
		100 ns	2	Glu 64, Asp 77
CD147_Lumacaftor	−10.6	0 ns	1	Glu 73
		20 ns	3	Lys 75, Glu 73, Lys 71
		40 ns	2	Lys 75, Glu 73
		60 ns	2	Lys 75, Glu 73
		80 ns	2	Lys 75, Lys 71
		100 ns	2	Lys 75, Glu 73
CD147_Pazopanib	−10.5	0 ns	2	Lys 75, Glu 64
		20 ns	1	Lys 75
		40 ns	1	Gln 70
		60 ns	2	Glu 84, Lys 57
		80 ns	3	Ser 130, Glu 129, Arg 106
			0	–

(*continued on next page*)

Table 1 (*continued*)

Complexes	Binding energy (kcal/mol)	H-bond Donor/ acceptor (0, 20, 40, 60, 80 and 100 ns)		H-bond Interactions (Interacting residues) (0, 20, 40, 60, 80 and 100 ns)
		100 ns		
RdRp _Rifabutin	−10.4	0 ns	1	Arg 553
		20 ns	1	Lys 551
		40 ns	2	Arg 836, Ile 548
		60 ns	1	Arg 836
		80 ns	3	Ile 548, Arg 555, Ser 549
		100 ns	1	Ile 548
RdRp_Dactinomycin	−10.2	0 ns	3	Asn 713, Asp 208, Arg 721
		20 ns	2	Asn 39, Asp 3
		40 ns		–
		60 ns	2	Lys 41, Ser 1
		80 ns	4	Lys 41, Tyr 728, Tyr 129, Arg 721
		100 ns	5	Arg 132, Asp 208, Leu 207, Lys 41,Asp 3
RdRp _Vancomycin	−10.2	0 ns	7	Ser 255, Val 320, Phe 321, Pro 461, Leu 460, Lys 391, Thr 393
		20 ns	5	Ser 255, Val 320, Asn 459, Pro 461, Phe 396
		40 ns	3	Asp 390, Asn 459, Val 320
		60 ns	6	Asp 390, Thr 393, Phe 396, Phe 321, Asn 459, Thr 319
		80 ns	8	Lys 391, Thr 393, Cys 395, Asn 459, Lys 263, Leu 261, Thr 319, Ser 318
		100 ns	9	Lys 391, Asp 390, Tyr 265, Thr 319, Asn 459, Asp 390, Thr 393, Arg 249, His 256
RdRp _Paritaprevir	−10	0 ns	2	Arg 624, Thr 556
		20 ns	1	Ala 554
		40 ns	2	Ala 554, Arg 836
		60 ns	1	Ala 554
		80 ns	2	Ala 554, Lys 621
		100 ns	2	Ala 554, Arg 858

complexes. The ACE2 complexes follow a similar trend in the MD trajectory like RdRp complexes, but CD147 complexes are different. The RMSF is explored to understand how the binding of drug molecules changes the behavior of the amino acid residues of the protein. A low RMSF is observed for the RdRp complexes, while ACE2 and CD147 complexes show high flexibility (Figs. 1B, 2B and 3B).

3.2.2. *The number of hydrogen bonds and free energy of interaction*

For further evaluations, the study utilized the MD simulation method to calculate the number of H-bonds and the amount of free energy of interaction. The number of H-bonds and free energy of interaction between ACE2, CD147, and RdRp and the drugs essential for stabilizing the complexes. The ACE2_vancomycin, ACE2_paritaprevir, CD147_estradiol, RdRp_vancomycin and RdRp-dactinomycin have the most hydrogen bonds over the 100 ns simulation time. Fig. 4 illustrated the number of H-bonds versus time at 310 K. The snapshots were generated at 0, 20, 40, 60, 80 and 100 ns, to investigate the stable hydrogen bonds between protein and ligands (Table 1). The figures of these complexes were drawn using Molegro Virtual Docker (The figures for hydrogen bonds in these intervals are provided in supplementary data). Tables 2–4 illustrate the calculation of ΔG for the polar & nonpolar interactions between protein and drugs, indicating that ledipasvir with ACE2, estradiol benzoate with CD147, vancomycin with RDRP had the most favorable ΔG.

4. Discussion

This study assessed the potential of FDA-approved small molecules to disrupt the interaction of virus-host cell components and interfere with the viral proliferation mechanism using drug repurposing approaches. The SARS-CoV-2 ACE2 receptor is integral in cardiovascular and renal diseases, diabetes, and lung injury [38]. Furthermore, the observations indicated that the expression of ACE2 correlated with the infection severity *in vitro* [15], which makes it a suitable candidate for pharmaceutical studies. Accordingly, many cases have been reported in which the administration of soluble ACE2 is observed as a competitive method for inhibiting virus binding to the host cell [39]. MD simulation results indicated that Ledipasvir with ACE2 had the most favorable ΔG (Table 2). Also, the results of molecular docking in a relevant study showed that Ledipasvir could interfere with the binding of S protein to ACE2 [40]. The stable binding energy during 100 ns MD simulations (−399.338 kcal/mol), together with RMSD and RMSF, confirm Ledipasvir inhibitory effects. Additionally, paritaprevir has good binding energy with both ACE 2 and RdRp targets. In this study, paritaprevir-ACE2 in 0–100 ns, Asp 206, have a key part in the hydrogen interactions during MD simulation (Table 1). Based on structural data, Asp 206 is located in the interaction surface with SARS-CoV-2 spike proteins [40]. Also, the complexes of ACE2 are stabilized by H-bonded interactions offered by residues that some of which are in the binding site [41]. The recent studies aiming at screening the FDA against SARS-CoV-2 proteins indicated that ledipasvir, paritaprevir, and simeprevir are promising medication candidates for COVID-19 treatment [42,43]. The clinical trials to evaluate the efficacy of ledipasvir in the treatment of COVID-19 are underway [44,45]. Ledipasvir and paritaprevir are direct-acting antiviral (DAA) medications used as part of combination therapy to treat chronic Hepatitis C, which is an infectious liver disease due to HCV infection. The RdRp enzyme is involved in viral genome replication and transcription of structural and peripheral small guided mRNAs (sgmRNAs) [46]. Therefore, it has been considered a primary target for many antiviral drugs, such as Remdesivir [5]. RdRp has conserved structural motifs like other polymerases, such as thumb (residues 816–932), palm (residues 860–815), and finger (residues 366–581) [47]. Vancomycin has the highest hydrogen bond with ACE2 and RdRp (Fig. 4). Also, MD simulation results indicated that vancomycin with RdRp had the most favorable ΔG (Table 4). In such a case, most of the residues involved in the interaction sites of the Vancomycin-RdRp complex, are located in the preferred conserved motifs and it was observed that Asn 459, Asp 390, Thr 393 and Lys 391 have strong hydrogen bonds in 100 ns simulation. Relevant studies show that vancomycin has the main part in infection treatment in severe coronavirus disease patients. Secondary bacterial infections associated with COVID-19 are caused by gram-positive bacteria, including methicillin-resistant *Staphylococcus aureus* (MRSA), methicillin-resistant, coagulase-negative staphylococci (MRCNS), and Enterococci species. These common nosocomial infections can cause ventilator-associated complications, like pneumonia, and are commonly treated with an antibiotic known as vancomycin. However, it has a narrow treatment window and some patients react differently to the drug leading to sub-optimal vancomycin concentrations in patients [48]. As you can see in Tables 2 and 4, sirolimus and dactinomycin also have suitable binding energy with ACE2 and RdRp. A recent study used a network-based drug repurposing sirolimus plus dactinomycin as

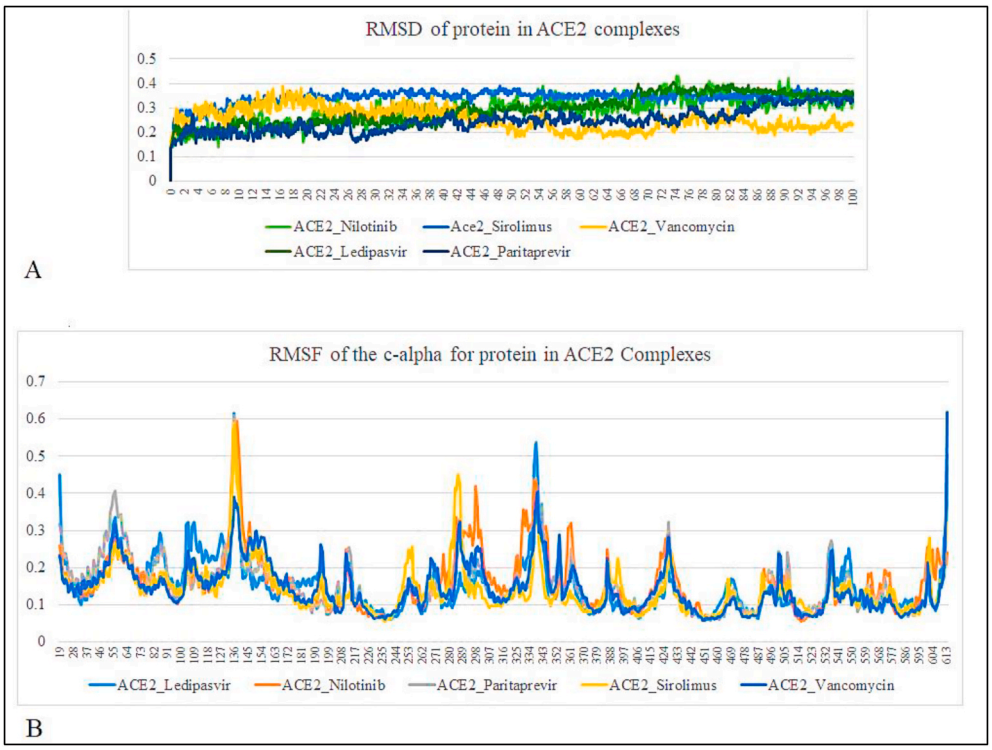

Fig. 1. A) Root mean square deviation (RMSD) for protein in ACE2 complexes B) Root mean square fluctuation (RMSF) for protein in ACE2 complexes.

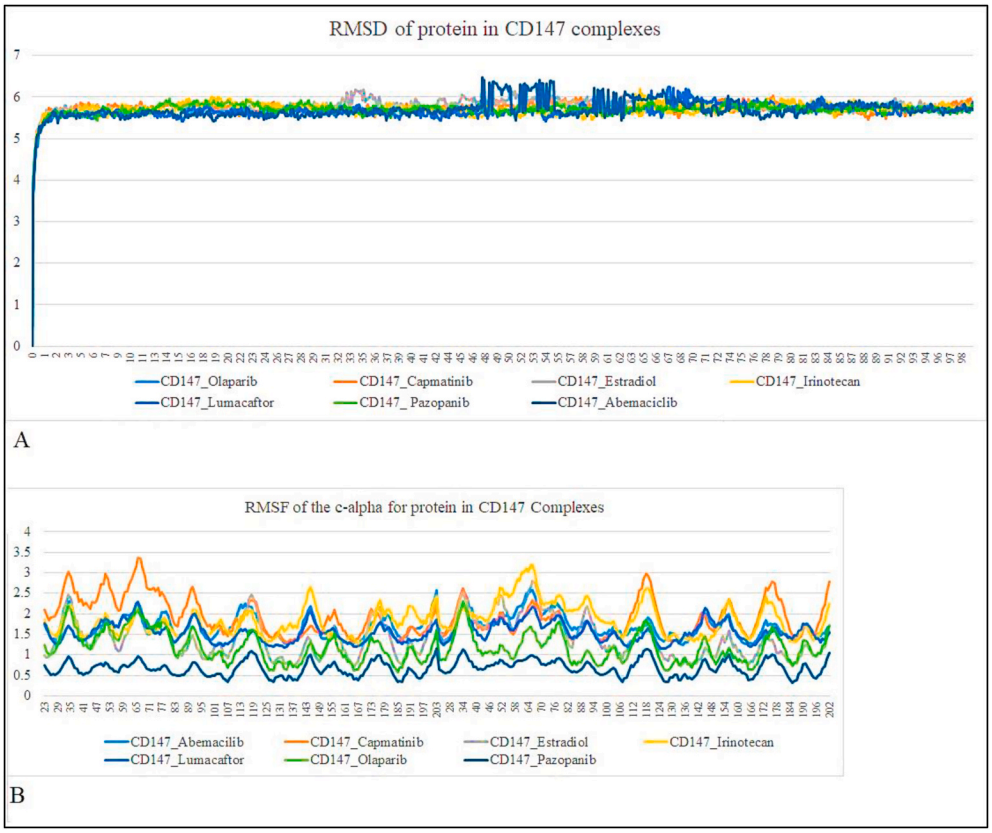

Fig. 2. A) Root mean square deviation (RMSD) for protein in CD147 complexes B) Root mean square fluctuation (RMSF) for protein in CD147 complexes.

treatment candidates for COVID-19 [49]. Nowadays, CD147 is regarded as an integral target in treating inflammatory diseases [50]. In 2016, a study investigated the role of small molecules in inhibiting CD147, which was used a Pharmacophore model derived from the structure of CD147. The results confirmed that the small molecule targeting CD147 was able to disrupt CD147 dimerization specifically and inhibit the

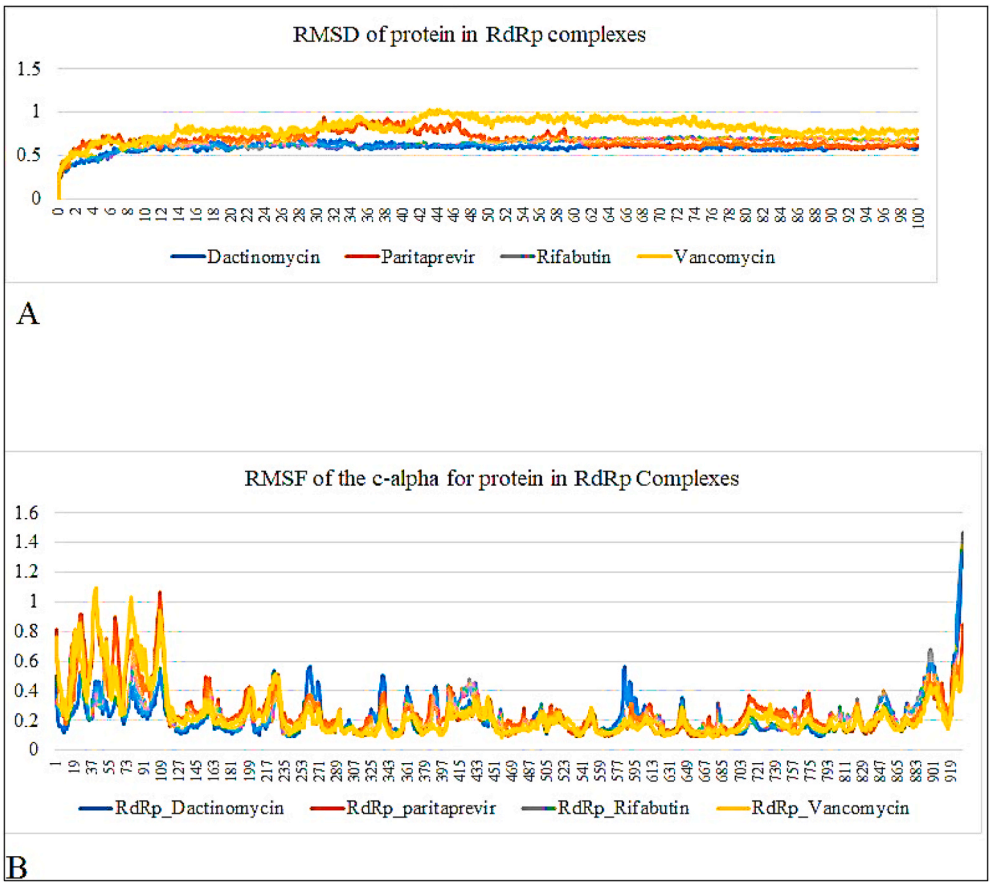

Fig. 3. A) Root mean square deviation (RMSD) for protein in RdRp complexes B) Root mean square fluctuation (RMSF) for protein in RdRp complexes.

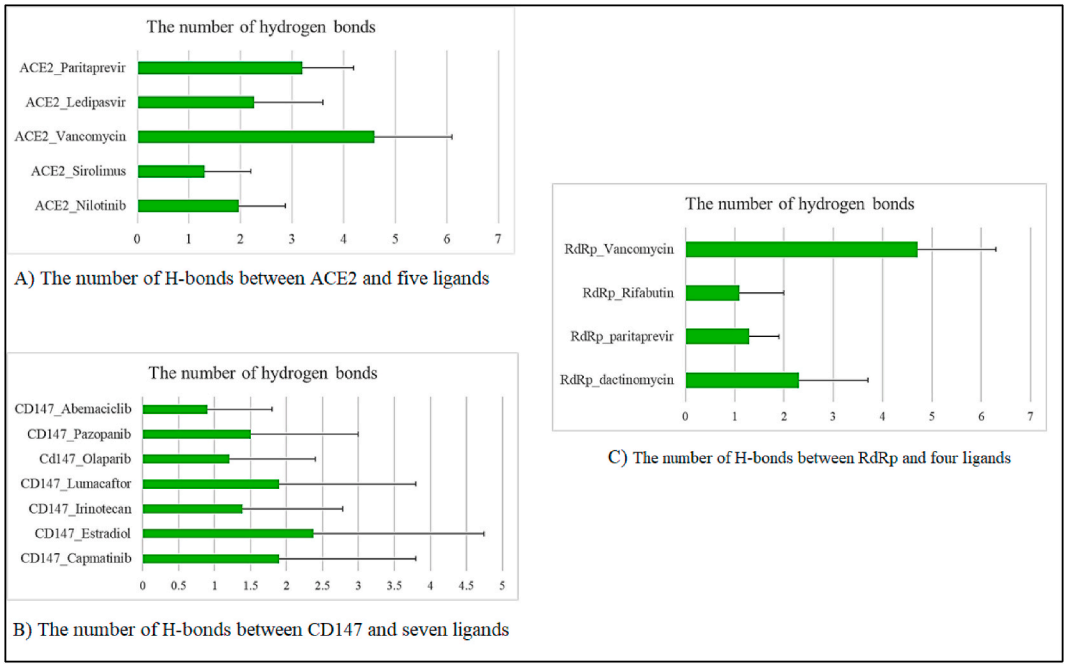

Fig. 4. A) The number of H-bonds between drugs and ACE2
B) The number of H-bonds between drugs and CD147
C) The number of H-bonds between drugs and RdRp.

Table 2
Calculation of binding free energy between ACE2 and five ligands.

Energetic analysis of ACE2_Paritaprevir binding (kcal/mol)	
Van der waals energy	−243.327 ± 20.169 kJ/mol
Electrostattic energy	−385.612 ± 45.807 kJ/mol
Polar solvation energy	278.425 ± 32.250 kJ/mol
SASA energy	−27.079 ± 1.613 kJ/mol
SAV energy	0.000 ± 0.000 kJ/mol
WCA energy	0.000 ± 0.000 kJ/mol
Binding energy	**−377.593 ± 27.965 kJ/mol**
Energetic analysis of ACE2_Ledipasvir binding (kcal/mol)	
Van der waals energy	−365.424 ± 28.481 kJ/mol
Electrostattic energy	−232.717 ± 41.105 kJ/mol
Polar solvation energy	237.007 ± 30.758 kJ/mol
SASA energy	−38.203 ± 2.670 kJ/mol
SAV energy	0.000 ± 0.000 kJ/mol
WCA energy	0.000 ± 0.000 kJ/mol
Binding energy	**−399.338 ± 34.121 kJ/mol**
Energetic analysis of ACE2_Vancomycin binding (kcal/mol)	
Van der waals energy	−265.305 ± 181.285 kJ/mol
Electrostattic energy	−176.105 ± 126.430 kJ/mol
Polar solvation energy	159.315 ± 112.978 kJ/mol
SASA energy	−30.433 ± 20.175 kJ/mol
SAV energy	0.000 ± 0.000 kJ/mol
WCA energy	0.000 ± 0.000 kJ/mol
Binding energy	**−312.528 ± 220.188 kJ/mol**
Energetic analysis of ACE2_Sirolimus binding (kcal/mol)	
Van der waals energy	−214.448 ± 13.337 kJ/mol
Electrostattic energy	−119.270 ± 22.811 kJ/mol
Polar solvation energy	126.964 ± 21.297 kJ/mol
SASA energy	−22.839 ± 1.853 kJ/mol
SAV energy	0.000 ± 0.000 kJ/mol
WCA energy	0.000 ± 0.000 kJ/mol
Binding energy	**−229.593 ± 19.460 kJ/mol**
Energetic analysis of ACE2_Nilotinib binding (kcal/mol)	
Van der waals energy	−235.239 ± 17.063 kJ/mol
Electrostattic energy	−128.180 ± 34.626 kJ/mol
Polar solvation energy	143.504 ± 24.681 kJ/mol
SASA energy	−24.062 ± 1.317 kJ/mol
SAV energy	0.000 ± 0.000 kJ/mol
WCA energy	0.000 ± 0.000 kJ/mol
Binding energy	**−243.978 ± 28.638 kJ/mol**

Table 3
Calculation of binding free energy between CD147 and seven ligands.

Energetic analysis of CD147_Irinotecan binding (kcal/mol)	
Van der waals energy	−174.593 ± 103.272 kJ/mol
Electrostattic energy	−55.686 ± 33.207 kJ/mol
Polar solvation energy	116.081 ± 48.658 kJ/mol
SASA energy	−17.337 ± 9.321 kJ/mol
SAV energy	0.000 ± 0.000 kJ/mol
WCA energy	0.000 ± 0.000 kJ/mol
Binding energy	**−131.535 ± 100.759 kJ/mol**
Energetic analysis of CD147_Abemaciclib binding (kcal/mol)	
Van der waals energy	−233.764 ± 50.730 kJ/mol
Electrostattic energy	−79.230 ± 41.013 kJ/mol
Polar solvation energy	149.647 ± 45.585 kJ/mol
SASA energy	−21.573 ± 4.408 kJ/mol
SAV energy	0.000 ± 0.000 kJ/mol
WCA energy	0.000 ± 0.000 kJ/mol
Binding energy	**−184.920 ± 48.393 kJ/mol**
Energetic analysis of CD147_Estradiol benzoate binding (kcal/mol)	
Van der waals energy	−131.767 ± 30.133 kJ/mol
Electrostattic energy	−178.810 ± 66.904 kJ/mol
Polar solvation energy	129.507 ± 33.693 kJ/mol
SASA energy	−16.980 ± 3.394 kJ/mol
SAV energy	0.000 ± 0.000 kJ/mol
WCA energy	0.000 ± 0.000 kJ/mol
Binding energy	**−198.051 ± 68.395 kJ/mol**
Energetic analysis of CD147_Capmatinib binding (kcal/mol)	
Van der waals energy	−145.146 ± 63.871 kJ/mol
Electrostattic energy	−192.172 ± 84.384 kJ/mol
Polar solvation energy	178.814 ± 80.230 kJ/mol
SASA energy	−16.781 ± 6.086 kJ/mol
SAV energy	0.000 ± 0.000 kJ/mol
WCA energy	0.000 ± 0.000 kJ/mol
Binding energy	**−175.286 ± 77.087 kJ/mol**
Energetic analysis of CD147_Olaparib binding (kcal/mol)	
Van der waals energy	−160.587 ± 28.548 kJ/mol
Electrostattic energy	−103.715 ± 36.951 kJ/mol
Polar solvation energy	119.027 ± 27.070 kJ/mol
SASA energy	−17.119 ± 2.583 kJ/mol
SAV energy	0.000 ± 0.000 kJ/mol
WCA energy	0.000 ± 0.000 kJ/mol
Binding energy	**−162.394 ± 40.148 kJ/mol**
Energetic analysis of CD147_Lumacaftor binding (kcal/mol)	
Van der waals energy	−135.172 ± 57.155 kJ/mol
Electrostattic energy	−62.656 ± 45.485 kJ/mol
Polar solvation energy	139.786 ± 41.844 kJ/mol
SASA energy	−15.503 ± 5.602 kJ/mol
SAV energy	0.000 ± 0.000 kJ/mol
WCA energy	0.000 ± 0.000 kJ/mol
Binding energy	**−73.545 ± 67.448 kJ/mol**
Energetic analysis of CD147_Pazopanib binding (kcal/mol)	
Van der waals energy	−124.506 ± 23.051 kJ/mol
Electrostattic energy	−66.763 ± 32.306 kJ/mol
Polar solvation energy	98.065 ± 19.386 kJ/mol
SASA energy	−12.842 ± 1.977 kJ/mol
SAV energy	0.000 ± 0.000 kJ/mol
WCA energy	0.000 ± 0.000 kJ/mol
Binding energy	**−106.046 ± 32.576 kJ/mol**

motility and invasion of hepatocellular carcinoma (HCC) cells [51]. Therefore, inhibition of CD147, with the help of small molecules, can play an effective role in treating some cancers and viral infections, including COVID-19. However, no small-molecule inhibitors for CD147 have been developed to date as an FDA-approved drug. A new study assessing the efficacy and safety of Meplazumab, a humanized anti-CD147 antibody, examined patients with SARS-CoV-2 pneumonia. Meplazumab efficiently improved the recovery of patients with COVID-19 pneumonia with a favorable safety profile [20]. These results support the inhibition of CD147 as a treatment host-targeted strategy for COVID-19 pneumonia. Besides, MD simulation results indicated that estradiol benzoate with CD147 had the most favorable ΔG. Estradiol Benzoate is a pro-drug ester of Estradiol, a naturally-occurring hormone that endogenously circulates within the human body. Estradiol is the most potent form of all mammalian estrogenic steroids and acts as the major female sex hormone. Recent results show that the risk of severe complications of COVID-19 is lower in women than in men. One of the reasons suggested by researchers is the high levels of estradiol in women (52, 53). In animal experiments, estrogen therapy suppressed inflammatory reactions and cured COVID-19 infection (54). Based on the results of this study, olaparib and irinotecan had a suitable free binding energy with CD147 (Table 3). A relevant study demonstrated that a combination of irinotecan (topoisomerase I inhibitor) and etoposide (a topoisomerase II inhibitor) can potentially inhibit cytokine storms in COVID-19 [52]. A type of clinical study using a drug repositioning strategy indicated the inhibitory effects of olaparib and mefuparib, as two PARP1 inhibitors, on COVID-19 [53]. Abemaciclib is an antitumor agent and dual inhibitor of cyclin-dependent kinases 4 (CDK4) and 6 (CDK6), that are involved in the cell cycle and promotion of cancer cell growth in case of unregulated activity.

5. Conclusion

The inhibition of CD147 and ACE2, as two main receptors of SARS-CoV-2, can prevent the entering of the virus into the host cells.

Table 4
Calculation of binding free energy between RdRp and four ligands.

Energetic analysis of RdRp _Rifabutin binding (kcal/mol)	
Van der waals energy	−255.358 ± 14.630 kJ/mol
Electrostattic energy	−86.179 ± 22.887 kJ/mol
Polar solvation energy	146.689 ± 31.438 kJ/mol
SASA energy	−24.834 ± 1.519 kJ/mol
SAV energy	0.000 ± 0.000 kJ/mol
WCA energy	0.000 ± 0.000 kJ/mol
Binding energy	**−219.682 ± 25.979 kJ/mol**
Energetic analysis of RdRp _Dactinomycin binding (kcal/mol)	
Van der waals energy	−255.358 ± 14.630 kJ/mol
Electrostattic energy	−86.179 ± 22.887 kJ/mol
Polar solvation energy	146.689 ± 31.438 kJ/mol
SASA energy	−24.834 ± 1.519 kJ/mol
SAV energy	0.000 ± 0.000 kJ/mol
WCA energy	0.000 ± 0.000 kJ/mol
Binding energy	**−219.682 ± 25.979 kJ/mol**
Energetic analysis of RdRp _Vancomycin binding (kcal/mol)	
Van der waals energy	−377.201 ± 20.328 kJ/mol
Electrostattic energy	−164.321 ± 39.955 kJ/mol
Polar solvation energy	187.785 ± 34.242 kJ/mol
SASA energy	−39.684 ± 1.918 kJ/mol
SAV energy	0.000 ± 0.000 kJ/mol
WCA energy	0.000 ± 0.000 kJ/mol
Binding energy	**−393.421 ± 29.051 kJ/mol**
Energetic analysis of RdRp _Paritaprevir binding (kcal/mol)	
Van der waals energy	−253.132 ± 25.403 kJ/mol
Electrostattic energy	−135.279 ± 26.412 kJ/mol
Polar solvation energy	193.800 ± 36.519 kJ/mol
SASA energy	−26.605 ± 2.695 kJ/mol
SAV energy	0.000 ± 0.000 kJ/mol
WCA energy	0.000 ± 0.000 kJ/mol
Binding energy	**−221.217 ± 23.556 kJ/mol**

Besides, the inhibition of RdRp, as the main enzyme for viral replication, is effective in fighting the COVID-19. Accordingly, this study aimed to use drug repurposing by virtual screening to identify inhibitors for CD147, ACE2, and RdRp. The results of this study showed that five drugs with ACE2, four drugs with RdRp, and seven drugs with CD147 achieved the most favorable free binding energy (Docking score < -10). These drugs were selected for MD simulation studies, the results of which indicated that ledipasvir with ACE2, estradiol benzoate with CD147, and vancomycin with RdRp had the most favorable ΔG. Drugs that can inhibit major virus receptors (ACE2 and CD147) were found to be effective in the early stages of viral infection, and inhibition of RdRp can also prevent disease progression. It was also shown for the first time in this study that, paritaprevir and vancomycin have good binding energy with both targets (ACE2 and RdRp). These drugs can be suitable candidates for further investigation as possible treatments of COVID-19 infection.

Funding sources

This research did not receive any specific grant from funding agencies in the public, commercial, or not-for-profit sectors.

Author contributions

Soodeh Mahdian collected and interpreted the data and prepared the manuscript. Yunes Panahi revised the manuscript and contributed to its design. Mahboobeh Zarrabi contributed to the design and revision of the manuscript, and Somayyeh Dabbagh contributed to the authorship of the manuscript.

Declaration of competing interest

The authors declare that they have no known competing financial interests or personal relationships that could have appeared to influence the work reported in this paper.

Acknowledgments

We are very grateful to all those who helped us with this project.

Appendix A. Supplementary data

Supplementary data to this article can be found online at https://doi.org/10.1016/j.imu.2021.100541.

References

[1] McCarthy JE, Dumas BA, McCarthy MT, Dewitt BD. A deterministic linear infection model to inform Risk-Cost-Benefit Analysis of activities during the SARS-CoV-2 pandemic. medRxiv 2020. https://doi.org/10.1101/2020.08.23.20180349.
[2] Lu Roujian, Zhao Xiang, Li Juan, Niu Peihua, Yang Bo, Wu Honglong, Wang Wenling, et al. Genomic characterisation and epidemiology of 2019 novel coronavirus: implications for virus origins and receptor binding. Lancet 2020;395 (10224). https://doi.org/10.1016/S0140-6736(20)30251-8.
[3] Geleris J, Sun Y, Platt J, Zucker J, Baldwin M, Hripcsak G, et al. Observational study of hydroxychloroquine in hospitalized patients with Covid-19. N Engl J Med 2020;382(25):2411–8. https://doi.org/10.1056/NEJMoa2012410.
[4] Gautret P, Lagier J-C, Parola P, Meddeb L, Mailhe M, Doudier B, et al. Hydroxychloroquine and azithromycin as a treatment of COVID-19: results of an open-label non-randomized clinical trial. Int J Antimicrob Agents 2020;56(1): 105949. https://doi.org/10.1016/j.ijantimicag.2020.105949.
[5] Shannon A, Le NT-T, Selisko B, Eydoux C, Alvarez K, Guillemot J-C, et al. Remdesivir and SARS-CoV-2: structural requirements at both nsp12 RdRp and nsp14 Exonuclease active-sites. Antivir Res 2020;178:104793. https://doi.org/10.1016/j.antiviral.2020.104793.
[6] Zauli G, Tisato V, Secchiero P. Rationale for considering oral Idasanutlin as a therapeutic option for COVID-19 patients. Front Pharmacol 2020;11. https://doi.org/10.3389/fphar.2020.01156.
[7] Cai Q, Yang M, Liu D, Chen J, Shu D, Xia J, et al. Experimental treatment with favipiravir for COVID-19: an open-label control study. Engineering 2020;6(10): 1192–8. https://doi.org/10.3389/fphar.2020.01156.
[8] Gordon DE, Jang GM, Bouhaddou M, Xu J, Obernier K, White KM, et al. A SARS-CoV-2 protein interaction map reveals targets for drug repurposing. Nature 2020; 583(7816):459–68. https://doi.org/10.1038/s41586-020-2286-9.
[9] Aftab Syed Ovais, Ghouri Muhammad Zubair, Masood Muhammad Umer, Haider Zeshan, Khan Zulqurnain, Ahmad Aftab, Munawar Nayla. Analysis of SARS-CoV-2 RNA-dependent RNA polymerase as a potential therapeutic drug target using a computational approach. J Transl Med 2020;18(1). https://doi.org/10.1186/s12967-020-02439-0.
[10] Kirchdoerfer Robert N, Ward Andrew B. Structure of the SARS-CoV Nsp12 polymerase bound to Nsp7 and Nsp8 Co-factors. Nat Commun 2019;10(1). https://doi.org/10.1038/s41467-019-10280-3.
[11] Andersen Kristian G, Rambaut Andrew, Lipkin W Ian, Holmes Edward C, Garry Robert F. The proximal origin of SARS-CoV-2. Nat Med 2020. https://doi.org/10.1038/s41591-020-0820-9.
[12] Yan Renhong, Zhang Yuanyuan, Li Yaning, Lu Xia, Guo Yingying, Zhou Qiang. Structural basis for the recognition of SARS-CoV-2 by full-length human ACE2. Science 2020;367(6485):1444–8. https://doi.org/10.1126/science.abb2762. 27.
[13] Wrapp Daniel, Wang Nianshuang, Corbett Kizzmekia S, Goldsmith Jory A, Hsieh Ching Lin, Abiona Olubukola, Graham Barney S, McLellan Jason S. Cryo-EM structure of the 2019-NCoV spike in the prefusion conformation. Science 2020;367 (6483):1260–3. https://doi.org/10.1126/science.abb2507. 13.
[14] Xue Xiaotong, Mi Zihao, Wang Zhenzhen, Zheng Pang, Liu Hong, Zhang Furen. High expression of ACE2 on keratinocytes reveals skin as a potential target for SARS-CoV-2. J Invest Dermatol 2021;141(1):206–9. https://doi.org/10.1016/j.jid.2020.05.087. e1.
[15] Zhuang Meng Wei, Cheng Yun, Zhang Jing, Xue Mei, Jiang, Wang Li, Deng Jian, Wang Pei Hui. Increasing host cellular receptor—angiotensin-converting enzyme 2 expression by coronavirus may facilitate 2019-NCoV (or SARS-CoV-2) infection. J Med Virol 2020;92(11):2693–701. https://doi.org/10.1002/jmv.26139.
[16] Cao Yanan, Lin Li, Feng Zhimin, Wan Shengqing, Huang Peide, Sun Xiaohui, Wen Fang, Huang Xuanlin, Ning Guang, Wang Weiqing. Comparative genetic analysis of the novel coronavirus (2019-NCoV/SARS-CoV-2) receptor ACE2 in different populations. Cell Discov 2020;24:6–11. https://doi.org/10.1038/s41421-020-0147-1.
[17] Valencia Inés, Peiró Concepción, Lorenzo Óscar, Sánchez-Ferrer Carlos F, Eckel Jürgen, Romacho Tania. DPP4 and ACE2 in diabetes and COVID-19: therapeutic targets for cardiovascular complications? Front Pharmacol 2020;11: 1161. https://doi.org/10.3389/fphar.2020.01161.

[18] Mahdian S, Shahhoseini M, Moini A. COVID-19 mediated by basigin can affect male and female fertility. Int J Fertil Steril 2020;14(3):262–3. https://doi.org/10.22074/ijfs.2020.134702.
[19] Muramatsu Takashi. Basigin (CD147), a multifunctional transmembrane glycoprotein with various binding partners. J Biochem 2016;159(5):481–90. https://doi.org/10.1093/jb/mvv127.
[20] Ulrich Henning, Pillat Micheli M. CD147 as a target for COVID-19 treatment: suggested effects of azithromycin and stem cell engagement. Stem Cell Rev Rep 2020;16(3):434–40. https://doi.org/10.1007/s12015-020-09976-7. 2020.
[21] Crosnier Cécile, Leyla Y, Bustamante S Josefin Bartholdson, Amy K, Bei, Theron Michel, Uchikawa Makoto, Mboup Souleymane, et al. Basigin is a receptor essential for erythrocyte invasion by Plasmodium falciparum. Nature 2011;9 (7378):534–7. https://doi.org/10.1038/nature10606. 480.
[22] Moheimani Fatemeh, Koops Jorinke, Williams Teresa, Reid Andrew T, Hansbro Philip M, Peter A Wark, Knight Darryl A. Influenza A virus infection dysregulates the expression of MicroRNA-22 and its targets; CD147 and HDAC4, in epithelium of asthmatics. Respir Res 2018;19(1):145. https://doi.org/10.1186/s12931-018-0851-7.
[23] Lan Jun, et al. Structure of the SARS-CoV-2 spike receptor-binding domain bound to the ACE2 receptor. Nature 2020;581(7807):215–20. https://doi.org/10.1038/s41586-020-2180-5.
[24] Yu XL, Hu T, Du JM, Ding JP, Yang XM, Zhang J, Chen ZN. Crystal structure of HAb18G/CD147: implications for immunoglobulin superfamily homophilic adhesion. J Biol Chem 2008;283(26):18056–65. https://doi.org/10.1074/jbc.M802694200.
[25] Bhattacharya D, Nowotny J, Cao R, Cheng J 3Drefine. An interactive web server for efficient protein structure refinement. Nucleic Acids Res 2016;44(W1):W406–9. https://doi.org/10.1093/nar/gkw336. 8.
[26] Wishart DS, Feunang YD, Guo AC, Lo EJ, Marcu A, Grant JR, Assempour N. DrugBank 5.0: a major update to the DrugBank database for 2018. Nucleic Acids Res 2018;46(D1):D1074–82. https://doi.org/10.1093/nar/gkx1037.
[27] Dallakyan S, Olson AJ. Small-molecule library screening by docking with PyRx, vol 1263. Humana Press; 2015. p. 243–50. https://doi.org/10.1007/978-1-4939-2269-7_19. Chemical Biology.
[28] Trott O, Olson AJ, Vina AutoDock. Improving the speed and accuracy of docking with a new scoring function, efficient optimization and multithreading. J Comput Chem 31 2010;31(2):455–61. https://doi.org/10.1002/jcc.21334.
[29] Hussein HA, Borrel A, Geneix C, Petitjean M, Regad L, Camproux AC. PockDrug-Server: a new web server for predicting pocket druggability on holo and apo proteins. Nucleic Acids Res 2015;43(W1):W436–42. https://doi.org/10.1093/nar/gkv462. Epub 2015 May 8.
[30] Bitencourt-Ferreira G, de Azevedo WF. Molegro virtual docker for docking. Methods Mol Biol 2019;2053:149–67. https://doi.org/10.1007/978-1-4939-9752-7_10.
[31] Berendsen HJC, van der Spoel D, van Drunen, Gromacs R. A message-passing parallel molecular dynamics implementation. Comput Phys Commun 1995;91: 43–56. https://doi.org/10.1016/0010-4655(95)00042-E.
[32] Best RB, Zhu X, Shim J, Lopes PEM, Mittal J, Feig M, MacKerell AD. Optimization of the additive charmm all-atom protein force field targeting improved sampling of the backbone Φ, Ψ and side-chain X (1) and X (2) dihedral angles. J Chem Theor Comput 2012;8(9):3257–73. https://doi.org/10.1021/ct300400x.
[33] P-Lincs Hess B. A parallel linear constraint solver for molecular simulation. J Chem Theor Comput 2008;4(1). https://doi.org/10.1021/ct700200b. 116-22.
[34] Hoover WG. Canonical dynamics: equilibrium phase-space distributions. Phys Rev 1985;31(3):1695–7. https://doi.org/10.1103/physreva.31.1695.
[35] Nosé S. A unified formulation of the constant temperature molecular dynamics methods. J Chem Phys 1984;81:511–9. https://doi.org/10.1063/1.447334.
[36] Parrinello M, Rahman A. Polymorphic transitions in single crystals: a new molecular dynamics method. J Appl Phys 1981;52:7182. https://doi.org/10.1063/1.328693.
[37] Kumari R, Kumar R, Lynn A, Lynn A. g_mmpbsa A GROMACS tool for high-throughput MM-PBSA calculations. J Chem Inf Model 2014;54:1951–62. https://doi.org/10.1021/ci500020m.
[38] Egieyeh S, Egieyeh E, Malan S, Christofells A, Fielding B. Computational drug repurposing strategy predicted peptide-based drugs that can potentially inhibit the interaction of SARS-CoV-2 spike protein with its target (humanACE2). PloS One 2021;16(1):e0245258. https://doi.org/10.1371/journal.pone.0245258.
[39] Behl T, Kaur I, Bungau S, Kumar A, Uddin MS, Kumar C, et al. The dual impact of ACE2 in COVID-19 and ironical actions in geriatrics and pediatrics with possible therapeutic solutions, vol. 257. Life Sciences; 2020. https://doi.org/10.1016/j.lfs.2020.118075. 257:118075.
[40] Miroshnychenko K, Shestopalova AV. Combined use of amentoflavone and ledipasvir could interfere with binding of spike glycoprotein of SARS-CoV-2 to ACE2: the results of molecular docking study. 2020 . https://doi.org/10.26434/chemrxiv.12377870.v1.
[41] Thuy BTP, My TTA, Hai NTT, Hieu LT, Hoa TT, Thi Phuong Loan H, Nhung NTA. Investigation into SARS-CoV-2 resistance of compounds in garlic essential oil. ACS Omega 2020;5(14):8312–20. https://doi.org/10.1021/acsomega.0c00772.
[42] Oliveira MD, Oliveira KM. Comparative docking of SARS-CoV-2 receptors antagonists from repurposing drugs. 2020. https://doi.org/10.26434/chemrxiv.12044538.v4.
[43] Mevada V, Dudhagara P, Gandhi H, Vaghamshi N, Beladiya U, Patel R. Drug repurposing of approved drugs elbasvir, ledipasvir, paritaprevir, velpatasvir, antrafenine and ergotamine for combating COVID19. 2020. https://doi.org/10.26434/chemrxiv.12115251.v1.
[44] Khalili H, Nourian A, Ahmadinejad Z, Jafari S, Sa DM, Rasolinejad M, Kebriaeezadeh A. Efficacy and safety of sofosbuvir/ledipasvir in treatment of patients with COVID-19; A randomized clinical trial. 2020 Acta Biomed: Atenei Parmensis 2020;91(4). https://doi.org/10.23750/abm.v91i4.10877. e2020102-e2020102.
[45] Pagliano P, Scarpati G, Sellitto C, Conti V, Spera AM, Ascione T, Filippelli A. Experimental pharmacotherapy for COVID-19: the latest advances. J Exp Pharmacol 2021;13:1. https://doi.org/10.2147/JEP.S255209.
[46] Sola I, Almazan F, Zuniga S, Enjuanes L. Continuous and discontinuous RNA synthesis in coronaviruses. Annu Rev Virol 2015;2:265–88. https://doi.org/10.1146/annurev-virology-100114-055218.
[47] Gao Y, Yan L, Huang Y, Liu F, Zhao Y, Cao L, Rao Z. Structure of the RNA-dependent RNA polymerase from COVID-19 virus. Science 2020;368(6492): 779–82. https://doi.org/10.1126/science.abb7498.
[48] Yin L, Qi T, Chen Y, Guo M, Shi H, Fan Y, Gao M. Pharmacokinetics and pharmacodynamics of vancomycin in severe COVID-19 patients: a preliminary study in a Chinese tertiary hospital. 2020. https://doi.org/10.21203/rs.3.rs-37635/v1.
[49] Zhou Y, Hou Y, Shen J, Huang Y, Martin W, Cheng F. Network-based drug repurposing for novel coronavirus 2019-nCoV/SARS-CoV-2. Cell Discov 2020;6(1): 1–18. https://doi.org/10.1038/s41421-020-0153-3.
[50] Zhu X, Song Z, Zhang S, Nanda A, Li G. CD147: a novel modulator of inflammatory and immune disorders. Curr Med Chem 2014;21(19). https://doi.org/10.2174/09298673216613227163352.
[51] Fu ZG, Wang L, Cuiv HY, Peng JL, Wangc SJ, Gengc JJ, et al. A novel small-molecule compound targeting CD147 inhibits the motility and invasion of hepatocellular carcinoma cells. Oncotarget 2016;7(8). https://doi.org/10.18632/oncotarget.6990.
[52] Lovetrue B. The AI-discovered etiology of COVID-19 and rationale of the Irinotecan + etoposide combination therapy for critically ill COVID-19 patients. Med Hypotheses 2020;144:110180. https://doi.org/10.1016/j.mehy.2020.110180.
[53] Ge Y, Tian T, Huang S, Wan F, Li J, Li S, Cheng L. A data-driven drug repositioning framework discovered a potential therapeutic agent targeting COVID-19. bioRxiv 2020. https://doi.org/10.1101/2020.03.11.986836.